Astronomy
&
Astrophysics

The stellar masses and specific star-formation rates of submillimetre galaxies⋆

M. J. Michałowski[1], J. S. Dunlop[1], M. Cirasuolo[1], J. Hjorth[2], C. C. Hayward[3], and D. Watson[2]

[1] SUPA⋆⋆, Institute for Astronomy, University of Edinburgh, Royal Observatory, Edinburgh, EH9 3HJ, UK
e-mail: mm@roe.ac.uk
[2] Dark Cosmology Centre, Niels Bohr Institute, University of Copenhagen, Juliane Maries Vej 30, 2100 Copenhagen Ø, Denmark
[3] Harvard-Smithsonian Center for Astrophysics, 60 Garden St., Cambridge, MA 02138, USA

ABSTRACT

Establishing the stellar masses, and hence specific star-formation rates of submillimetre galaxies is crucial for determining the role of such objects in the cosmic history of galaxy/star formation. However, there is as yet no consensus over the typical stellar masses of submillimetre galaxies, as illustrated by the widely differing results reported from recent optical-infrared studies of submillimetre galaxies with spectroscopic redshifts $z \simeq 2$–3. Specifically, even for the same set of submillimetre galaxies, the reported average stellar masses have ranged over an order of magnitude, from $\simeq 5 \times 10^{10}\,M_\odot$ to $\simeq 5 \times 10^{11}\,M_\odot$. Here we study how different methods of analysis can lead to such widely varying results. We find that, contrary to recent claims in the literature, potential contamination of IRAC 3–8 μm photometry from hot dust associated with an active nucleus is not the origin of the published discrepancies in derived stellar masses. Instead, we expose in detail how inferred stellar mass depends on assumptions made in the photometric fitting, and quantify the individual and cumulative effects of different choices of initial mass function, different "brands" of evolutionary synthesis models, and different forms of assumed star-formation history. We review current observational evidence for and against these alternatives as well as clues from the hydrodynamical simulations, and conclude that, for the most justifiable choices of these model inputs, the average stellar mass of luminous ($S_{850} \gtrsim 5$ mJy) submillimetre galaxies is $\simeq 2 \times 10^{11}\,M_\odot$ to within a factor $\simeq 2$. We also check and confirm that this number is perfectly reasonable in the light of the latest measurements of the dynamical masses of these objects ($\simeq 2$–$6 \times 10^{11}\,M_\odot$ from CO (1–0) observations), and the evolving stellar mass function of the overall galaxy population. Galaxy stellar masses of this order imply that the average specific star-formation rate of submillimetre galaxies is comparable to that of other star-forming galaxies at $z > 2$, at 2–3 Gyr^{-1}. This supports the view that, while rare outliers may be found at any stellar mass, most submillimetre galaxies simply form the top end of the "main-sequence" of star-forming galaxies at these redshifts. Conversely, this argues strongly against the viewpoint, frequently simply asserted in the literature, that submillimetre galaxies are extreme pathological objects, of little relevance in the cosmic history of star-formation.

Key words. galaxies: active – galaxies: evolution – galaxies: high-redshift – galaxies: ISM – galaxies: starburst – submillimeter: galaxies

1. Introduction

The properties of galaxies selected at submillimetre wavelengths (SMGs) have yet to be fully understood. In particular, there is still no real consensus over their stellar masses. A robust measurement of the stellar masses of SMGs is key to addressing a number of important issues, including the evolution of the relationship between galaxy and black-hole masses (Borys et al. 2005; Hainline et al. 2011, H11 thereafter), and the contribution of SMGs to the overall history of stellar mass assembly (Michałowski et al. 2010a, M10 hereafter). Perhaps most importantly, a proper understanding of the stellar masses of SMGs is required to distinguish whether their massive dust-enshrouded star-formation rates are fuelled primarily by mergers, or by cold gas infall (Swinbank et al. 2008; Davé et al. 2010; González et al. 2011; Narayanan et al. 2010b; Ricciardelli et al. 2010; Hayward et al. 2011a,b, 2012). Unless the uncertainty in stellar masses can be reduced, it is in essence impossible to tell whether SMGs have specific star-formation rates (sSFR = SFR/M_*) comparable

to those of other star-forming galaxy populations at $z > 2$, or whether they are extreme outliers from the "main-sequence" of star-forming galaxies (Daddi et al. 2007; Noeske et al. 2007; González et al. 2010).

Most previous studies of the stellar masses of SMGs have concluded in favour of values in the range $\simeq 10^{11}$–$10^{12}\,M_\odot$ (Borys et al. 2005; Dye et al. 2008). However, two recent studies of $\simeq 70$ SMGs with spectroscopic redshifts $\simeq 2$–3 from Chapman et al. (2005) have reached apparently very different conclusions, highlighting the impact of alternative methods of analysis. Specifically, Michałowski et al. (2010a,b) found stellar masses consistent with previous studies, with a median value $M_* = 3.5 \times 10^{11}\,M_\odot$ (see also Hatsukade et al. 2010; Ikarashi et al. 2011; Santini et al. 2010; Tamura et al. 2010), whereas Hainline et al. (2011) have reported values, based on *the same* SMGs, which are systematically lower by a factor of $\simeq 6$ (median $M_* = 5$–$7 \times 10^{10}\,M_\odot$; see also Wardlow et al. 2011).

The primary objective of this paper is to explore the origins of this discrepancy, and to attempt to resolve it. More generally, however, we have taken this opportunity to expose in detail how the derived stellar masses (and hence sSFRs) of SMGs depend on different assumed forms of star-formation history, and

---

⋆ Appendix A is available in electronic form at
http://www.aanda.org
⋆⋆ Scottish Universities Physics Alliance.

different "brands" of evolutionary synthesis models. The use of a sample of SMGs with spectroscopic redshifts is especially useful for this purpose, since it is well known that, if only photometric redshifts are available, the errors in derived stellar masses can be dominated by the effect of uncertainties in z_{phot}.

The structure of this paper is as follows. In Sect. 2 we delineate the various factors and choices of analysis methods which influence the stellar mass determinations and quantify their impact on the final derived values. We also review recent evidence that informs the preferred choice of, for example, initial mass function (IMF) and evolutionary synthesis model, and conclude that for most reasonable choices of such model inputs the derived stellar masses in fact only differ by a factor $\simeq 2$. In Sect. 3 we investigate the consistency of our re-derived stellar masses with the latest measurements of the dynamical masses of these objects, the evolving stellar mass function of the overall galaxy population, and the predictions of theoretical simulations. We discuss the implications of our results on the sSFR of SMGs in Sect. 4, and close with a summary of our conclusions in Sect. 5. We use a cosmological model with $H_0 = 70\,\mathrm{km\,s^{-1}\,Mpc^{-1}}$, $\Omega_\Lambda = 0.7$ and $\Omega_m = 0.3$.

2. Determining the stellar masses of SMGs

2.1. Initial mass function

The choice of a particular IMF introduces a systematic uncertainty of a factor of $\simeq 2$ in the determination of the stellar masses (M_*) and star-formation rates (SFRs; Erb et al. 2006). Specifically, the differences between the IMFs assumed by M10 (Salpeter 1955) and H11 (Chabrier 2003) accounts for a factor of 1.8 in the difference between the quoted stellar mass estimates.

Both top-heavy and standard IMFs have been claimed to reproduce the number counts of SMGs (Baugh et al. 2005; Fontanot et al. 2007; Hayward et al. 2011b). This confusing situation is further exacerbated by the fact that different studies of local ellipticals (arguably the likely present-day descendants of SMGs) have yielded a wide range of preferred IMFs including bottom-light (van Dokkum 2008), Kroupa (2001) (Gerhard et al. 2001; Cappellari et al. 2006), Salpeter (Grillo et al. 2009), and even bottom-heavy (van Dokkum & Conroy 2010, 2011; see also Thomson & Chary 2011).

Hence, since there is as yet no clear evidence that the IMF of SMGs is systematically different from that of other galaxies, in this paper we assume the Chabrier (2003) IMF (unless stated otherwise) to which all appropriate derived quantities are converted if necessary (values derived using the Salpeter 1955 IMF are divided by 1.8). This IMF has been derived for the Milky Way and represents an intermediate choice between the top-heavy and the bottom-heavy IMFs. We also note that this "Chabrier IMF" is essentially identical to the "Canonical IMF" recently summarised by Weidner et al. (2011). While we argue that this IMF is the natural choice on the basis of current evidence, it must still be accepted that we must live with a fundamental uncertainty of $\simeq \times 2$ in stellar masses until the uncertainty in the IMF in SMGs is resolved. However, we also note that the derived sSFR is unaffected by this IMF uncertainty, making it a particularly useful quantity for comparing the properties of different types of star-forming galaxies.

2.2. Evolutionary models and star-formation histories

It is well known that the choice of the evolutionary synthesis model used to fit the optical-infrared photometry can affect
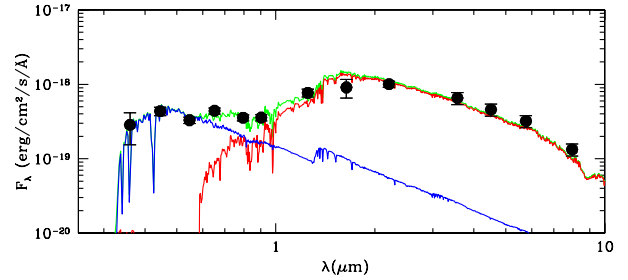
Fig. 1. Spectral energy distribution (flux density vs. observed wavelength) of SMMJ123606.85+621021.4 at the spectroscopic redshift $z = 2.509$ fitted using the double-component star formation history method of Cirasuolo et al. (2010, C10). *Black circles* denote the data, *red and blue curves* are the SEDs of the old and young components, respectively, and the *green curve* is the sum of these two components. The older component dominates the near-IR light and the derived stellar mass, whereas the young component delivers almost all rest-frame ultraviolet flux density.

the derived stellar masses of any type of galaxy. The GRASIL spectral energy distribution (SED) templates (Silva et al. 1998; Iglesias-Páramo et al. 2007) used by M10 make use of the Padova stellar tracks (Alongi et al. 1993; Bressan et al. 1993; Bertelli et al. 1994; Fagotto et al. 1994a,b,c; Girardi et al. 1996, 2000). The input metallicity for GRASIL was calculated based on the chemical evolution model in which individual stellar populations are allowed to have metallicity between 0.2–5 $Z_\odot$. The mean (median) metallicity derived for SMGs is 0.8 $Z_\odot$ (0.6 $Z_\odot$).

H11 used Bruzual & Charlot (2003) models (which are also based on the Padova library) and in addition explored the use of the Maraston (2005) models. H11 assumed solar metallicity in order to derive a typical mass-to-light ratio.

The stellar masses derived by H11 using Bruzual & Charlot (2003) models are on average $\simeq 50\%$ higher than those calculated using the Maraston (2005) models. This average difference is at least in part a consequence of the higher contribution of thermally pulsing asymptotic giant branch (TP-AGB) stars in the Maraston (2005) models, which reduces the derived mass-to-light ratio at rest-frame near-infrared wavelengths at stellar population ages $\simeq 1$ Gyr (a point discussed further below).

An apparently separate (but, it transpires, in fact connected) cause of differing stellar mass estimates is the chosen parameterisation of the star-formation histories (SFHs) of the galaxies in question. As noted by H11, due to their high redshift, and often rather red spectral-energy distributions, it is very difficult to recover robust SFHs for SMGs from photometric data (cf. Dye et al. 2008, 2010). This leads inevitably to difficulty in constraining galaxy ages and mass-to-light ratios.

In an attempt to account for this uncertainty, H11 explored the use of two alternative single-component SFHs, adopting either an instantaneous starburst or a continuous star-formation history. H11 then averaged the two resulting estimates to produce the adopted stellar mass for each galaxy. In contrast, M10 assumed a two-component SFH consisting of a smooth Schmidt-type law ($SFR \propto M_{gas}$) with a recent starburst superimposed commencing 50 Myr before the observed galaxy SED was emitted, and with a mass in the range 0–9% of the infalling gas mass.

The assumption of a multi-component SFH generally naturally leads to higher mass-to-light ratios and, in turn, higher stellar masses than the use of a single-component model. This is because, while the starburst component can account for the ultraviolet (UV) emission (and the infrared emission from the UV-heated dust), the second (older) component is then free to
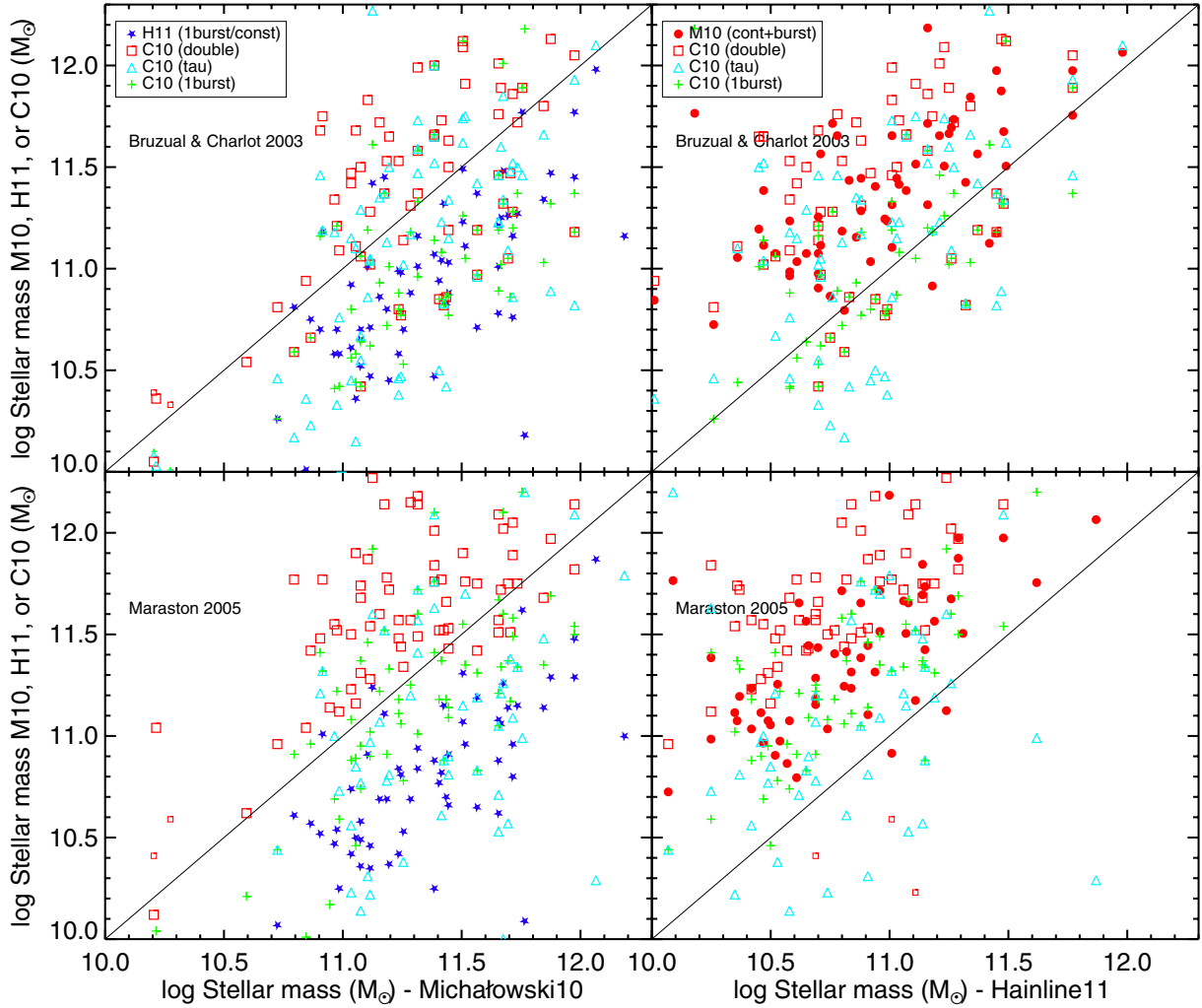
Fig. 2. Comparison of the stellar masses of SMGs as derived by M10, H11 and in the present work using the stellar population synthesis models of Bruzual & Charlot (2003, *top)* and Maraston (2005, *bottom)*. The different symbols indicate the stellar masses derived by M10 (*red circles*), H11 (*blue stars*), and our new estimates based on the SED modelling method of Cirasuolo et al. (2010, C10) for three alternative forms of star formation history: double component model (*red squares*), exponentially declining tau model (*light blue triangles*) and single burst (*green pluses*). All the derived masses have been converted to the Chabrier (2003) IMF. Small symbols denote $z < 0.5$ SMGs. The M10 stellar masses are consistent with our new estimates for the double-component models, whereas the H11 stellar masses are consistent with single component models, and are on average a factor of $\simeq 2.5$ smaller than the double-component estimates (see Table 1).

contribute more stars with higher mass-to-light ratios (see Fig. 1 and also Schael et al., in prep.). By contrast, the use of a single instantaneous starburst model limits the age of the *entire* stellar population to the young age of the starburst required to match the UV emission (and thus the true stellar masses are inevitably under-estimated), while in the continuous star-formation model the current SFR is set by the UV emission and the total age is then limited in order not to overshoot the optical and the near-IR part of the spectrum (assuming the galaxy has always formed stars at the same high rate).

In order to further clarify the impact of the choice of stellar population synthesis models and star-formation histories on the derived stellar masses we have revisited the SED fitting of the Chapman et al. (2005) SMG sample. Specifically, we have used the method presented in Cirasuolo et al. (2007, 2010), based on the HYPERZ package utilising both Bruzual & Charlot (2003) and Maraston (2005) models and assuming three different forms of SFH: an instantaneous burst of star-formation, an exponentially declining star-formation rate (so-called tau models), and a double-component model composed of two instantaneous

bursts with different ages and (independent) dust attenuations (an example is shown in Fig. 1 and all estimates are listed in Table A.1). In the double-component model the age of the young component was varied between 50 Myr and 1.5 Gyr, and the old component was allowed to contribute 0–100% of the near-IR emission while its age was varied over the range 1–6 Gyr. Solar metallicity was assumed. These models were run using the Chabrier IMF.

The results of this modelling are illustrated in Fig. 2 and summarised in Table 1, where the mean and median values of M_* and sSFR (as well as ages and contributions of the older population) for the SMGs are tabulated for the full range of different stellar population synthesis models and star-formation histories explored in M10, H11 and the present work (it is not possible to distinguish the models based on the goodness of fit). What is immediately evident from this table is that the results are strongly dependent on the assumed parameterisation of the star-formation history (see also Bussmann et al. 2012), as is the impact of assuming different population synthesis models. In particular, it is noteworthy that the Maraston (2005) models only result in

Table 1. Comparison of stellar masses and specific star formation rates of SMGs calculated using various methods, stellar population models and star formation histories.

Fit[a]	SSP[b]	SFH[c]	Mean M_* (log $M_\odot$)	Median M_* (log $M_\odot$)	Mean SSFR (Gyr^{-1})	Median SSFR (Gyr^{-1})	Age$_Y$[d] (Gyr)	Age$_O$[e] (Gyr)	Frac$_O$[f]
M10	Padova	cont+burst	11.32 ± 0.05	$11.31^{+0.07}_{-0.06}$	2.86 ± 0.43	$1.74^{+0.17}_{-0.46}$	0.050	1.856	0.84
H11	BC03	1burst/const	10.87 ± 0.06	$10.88^{+0.11}_{-0.07}$	9.71 ± 1.99	$4.60^{+1.22}_{-0.92}$	0.820	$\cdots$	$\cdots$
H11	M05	1burst/const	10.71 ± 0.06	$10.74^{+0.08}_{-0.05}$	12.96 ± 2.17	$6.85^{+1.56}_{-2.09}$	0.860	$\cdots$	$\cdots$
C10	BC03	double	11.44 ± 0.08	$11.47^{+0.11}_{-0.10}$	10.87 ± 8.68	$1.35^{+0.21}_{-0.31}$	0.191	1.332	0.87
C10	BC03	tau	11.16 ± 0.10	$11.18^{+0.11}_{-0.05}$	17.36 ± 11.98	$2.56^{+1.00}_{-0.71}$	1.178	$\cdots$	$\cdots$
C10	BC03	1burst	11.06 ± 0.10	$11.02^{+0.06}_{-0.06}$	14.88 ± 8.69	$3.07^{+1.16}_{-0.47}$	0.246	$\cdots$	$\cdots$
C10	M05	double	11.73 ± 0.06	$11.72^{+0.03}_{-0.12}$	1.25 ± 0.19	$0.67^{+0.25}_{-0.11}$	0.075	1.777	0.66
C10	M05	tau	10.46 ± 0.13	$10.78^{+0.07}_{-0.17}$	167.34 ± 47.42	$5.16^{+6.38}_{-0.78}$	0.767	$\cdots$	$\cdots$
C10	M05	1burst	11.24 ± 0.07	$11.22^{+0.12}_{-0.04}$	8.43 ± 4.57	$1.90^{+0.49}_{-0.43}$	0.198	$\cdots$	$\cdots$

Notes. The Chabrier (2003) IMF is assumed. Errors are standard deviations for the means and bootstrap 68% ranges for medians. [a] SED fitting method presented in M10 (Michałowski et al. 2010a), H11 (Hainline et al. 2011), or C10 (Cirasuolo et al. 2010). [b] Single stellar population models being either Padova tracks, BC03 (Bruzual & Charlot 2003) or M05 (Maraston 2005). [c] Assumed star formation history being either a continous SFH with a burst (cont+burst), an average of the single burst and constant (1 burst/const), double burst (double), single burst (1 burst), or exponentially declining (tau). [d] Mean age of the younger stellar component. [e] Mean age of the older stellar component. [f] Mean fractional contribution to the total stellar mass of the older component.

significantly lower stellar masses (and hence substantially higher sSFRs) than the Bruzual & Charlot (2003) models when a single-component exponentially-declining tau-model SFH is assumed. We investigated the origin of this effect, and found that, when allowed only single-component tau models, the mean preferred age of the Maraston (2005) model fits is ≃0.8 Gyr (see Table 1), which corresponds closely to the time at which the enhanced TP-AGB star contribution in the Maraston (2005) models has maximum impact. This result provides further evidence that the combination of tau SFHs and the Maraston (2005) models is not appropriate for SMGs.

Reassuringly, however, there is no significant difference between the masses derived with these two alternative models for a single burst SFH. This is because, in order to reproduce the star-forming nature of SMGs, the single burst fitting typically results in much younger ages of ≃0.2 Gyr, corresponding to the time when the TP-AGB contribution is small and does not have a significant influence on the derived stellar masses.

As expected (see above discussion of the M10 modelling approach), the stellar masses obtained using the double component SFH are systematically larger. Especially, the Maraston (2005) models with the double SFH yield stellar masses higher by ≃1 dex than these derived assuming the tau SFHs with these models.

In summary, the derived stellar masses depend primarily on the assumed parameterisation of the SFH, and the different evolutionary synthesis models only yield significantly different results if the single-component exponentially-declining SFH is adopted (due primarily to the extreme behaviour of the Maraston 2005, models with this adopted parameterization of SFH). Since, as we argue below, a model of a rapidly starforming galaxy in which the SFR is assumed to have been even higher at *all* previous epochs is obviously physically unrealistic for SMGs, the preferred choice of evolutionary synthesis model is actually of less importance in deriving the stellar masses of SMGs than might have been supposed. Nevertheless, in the next section, we do, for completeness, review the arguments for and against the choice of the Maraston (2005) or Bruzual & Charlot (2003) models.

Of more significance is the fact that, as can be seen from Table 1, our new two-component models using the

Bruzual & Charlot (2003) models yield a value very similar to that derived by M10 using a *different* form of two-component model, and a different evolutionary synthesis model (albeit based on the same stellar tracks as the Bruzual & Charlot 2003 models). Thus, consistent average stellar masses are produced by models which allow recent and past SFR to be decoupled, regardless of whether the earlier star-formation is parametrised as a single burst or a more extended period of star formation. This consistency is both reassuring and helpful given that, as we argue further below, a SFH history allowing potentially decoupled recent and past star-formation activity is rather obviously appropriate for objects selected on the basis of recent very violent star formation within an already metal enriched environment.

2.3. Choice of evolutionary synthesis model

Recent years have seen some vigorous debate over whether the stronger TP-AGB contribution introduced into evolutionary synthesis models by Maraston (2005) is justified by the data.

Some workers have argued for the superiority of the Maraston (2005) models based on derived galaxy stellar masses (van der Wel et al. 2006a,b), on derived photometric redshifts (Maraston et al. 2006), on average broad-band SEDs (Maraston et al. 2006; Cimatti et al. 2008), on optical and near-infrared colours (MacArthur et al. 2010), and by comparison with semi-analytical models (Henriques et al. 2011). Moreover, Zibetti et al. (2009) have claimed that stellar mass determinations based on i- and H-band luminosities are more consistent with each other when long-lived TP-AGB stars are introduced.

However Eminian et al. (2008) showed that Maraston (2005) models predict excessively red optical colours, and recently Kriek et al. (2010) have found that the average spectral energy distribution of post-starburst galaxies at $0.7 \lesssim z \lesssim 2.0$ does not appear to display the excess near-infrared flux predicted from the TP-AGB contribution in the Maraston (2005) models. Indeed, they demonstrate that the Bruzual & Charlot (2003) model provides a much better description of the the data, even at the age when the TP-AGB contribution should be near maximum. In addition, Conroy & Gunn (2010, their Figs. 2 and 16) have found that the Maraston (2005) models predict excessively red colours

for post-starburst galaxies and for star clusters in the Magellanic Clouds. Finally, Zibetti et al. (2012) did not find any strong carbon feature of TP-AGB stars in the near-IR spectra of post-starburst galaxies.

The work presented here cannot be used to definitively resolve this issue, but we note that the extreme outlying nature of the tau-model Maraston (2005) results shown in Table 1 arguably provides some further evidence against the plausibility and appropriateness of the strong TP-AGB contribution adopted in these models for tau SFHs. Moreover, we note that the Maraston (2005) models with the double SFH yield the highest median stellar masses for SMGs.

We also note that, confining the comparison to the use of the Chabrier (2003) IMF and the Bruzual & Charlot (2003) models, the median stellar mass of SMGs derived by M10 ($M_* = 2 \times 10^{11} M_\odot$) is in fact only a factor of $\simeq 2.5$ higher than that reported by H11 ($M_* = 7.6 \times 10^{10} M_\odot$).

2.4. Choice of star-formation history

The key issue for stellar mass determination, therefore, appears to be the choice of how to parameterize the SFH of SMGs. Reassuringly, however, the results do not appear to be very sensitive to precisely how this is parameterized, provided the SFH allows past and "present" star-formation activity to be, at least in principle, disconnected. This can be seen from the fact that the different two-component models based on the Padova tracks listed in Table 1 yield average stellar masses in the range $M_* = 2{-}3 \times 10^{11} M_\odot$.

It only therefore remains to consider if these two-component models should be preferred to single-component burst or tau models. In fact, at least for SMGs, this is a relatively straightforward argument, since both the single-burst and tau models both enforce the condition that the star-formation rates in SMGs were always higher at epochs earlier than that at which the object has been selected due to its extreme star-formation rate. Indeed this problem has already been discussed by several authors including Maraston et al. (2010). They concluded that, for high-redshift galaxies, the assumption of an exponentially decreasing SFH (as well as constant SFH to some extent) leads to unrealistically low ages and under-estimated stellar masses, because the SED fit is completely dominated by young stars. In fact Maraston et al. (2010) found an exponentially *increasing* SFH could provide a much better description of data. Such SFHs are conceptually similar to those used in M10, with the SFR being highest close to the epoch at which the observed galaxy SED was emitted, and indeed there is growing evidence in favour of rising SFHs in the wider population of galaxies studied at high redshift (e.g. Finlator et al. 2011; Papovich et al. 2011).

The lack of either two-component models or rising SFHs in the analysis of H11 (or indeed Wardlow et al. 2011) can therefore explain all of the remaining discrepancy in the average stellar masses reported by M10 and H11 since, as can be seen from Table 1, the use of a double component SFH results in stellar masses of SMGs being $\simeq 3$ times larger than that deduced using the single burst model and $\simeq 2$ times larger than that derived using the tau models. This is also illustrated in Fig. 2, where the masses derived assuming single-component SFHs (light blue triangles and green plusses) are systematically lower than those derived assuming the more realistic double-component SFHs (red squares). This conclusion is consistent with the findings of Schael et al. (in prep.)[1] who found that the stellar masses of

---

[1] See also Schael (2009).

the SHADES SMGs (Coppin et al. 2006) derived using a two-component SFH are on average a factor of $\simeq 2{-}3$ higher than when derived using a single-component SFH.

2.5. Other model-fitting issues

2.5.1. Wavelength range

The wavelength range used in the SED model fitting could potentially affect the resulting derived stellar masses. For completeness we therefore tested whether the difference in the SMG stellar mass estimates derived by M10 and H11 is not, at least in part, due to the fact that M10 fitted the entire multi-frequency dataset up to radio wavelengths, whereas H11 confined attention to observed $\lambda \le 8.0\,\mu m$. To test this we simply repeated the analysis performed by M10, but this time restricting the model fitting to photometry at optical, near-infrared and IRAC wavelengths. We obtained almost identical results with a median stellar mass of $\simeq 1.7 \times 10^{11} M_\odot$ instead of $\simeq 1.9 \times 10^{11} M_\odot$, and hence conclude that the longer-wavelength data have no significant influence on the derived stellar masses. This is reassuring and is easily explained since the emission at far-infrared wavelengths depends only on the properties of the dust and of the younger stellar population that is heating the dust, and should be essentially unaffected by the older stars which dominate the total stellar masses of SMGs (M10).

2.5.2. AGN contamination

SMGs are believed to suffer only a minor ($\simeq 10{-}30\%$) contamination of their bolometric luminosities by active galactic nuclei (AGNs; Alexander et al. 2005, 2008; Menéndez-Delmestre et al. 2007, 2009; Valiante et al. 2007; Pope et al. 2008; Hainline et al. 2009; Murphy et al. 2009; Watabe et al. 2009, M10). Here we consider whether the presence of AGNs in SMGs can significantly influence the derivation of their typical stellar masses.

H11 reported that, for $\simeq 50\%$ of SMGs, non-stellar (AGN) power-law features contribute $<10\%$ in the rest-frame H-band, whereas, for $\simeq 10\%$ of SMGs, the contribution is $>50\%$. However, even for those objects which do appear to have a significant AGN contribution at observed IRAC wavelengths, it is not obvious that the stellar masses based on our full multi-wavelength fitting will be significantly distorted, especially given the typically large ($\simeq 20\%$) photometric errors generally assigned to IRAC data in the SED fitting process. In fact we find that the stellar masses reported by H11 are consistent with our estimates for single component models (Fig. 2 and Table 1), without making any corrections for possible AGN contributions. We therefore do not find any evidence to support the idea that the lower stellar masses reported by H11 are due to the subtraction of an AGN component. Rather, as described above, it seems clear that the lower stellar masses deduced by H11 arise, primarily, from the adoption of a single-component SFH.

We also note that the presence of any power-law features in the IRAC data should not have strongly affected the mass estimates of M10, simply because the SED fits were not forced to reproduce the power-law features and, in fact, the best-fitting stellar models tend to under-estimate the longer wavelength IRAC data when the power-law component appears to be present (see Fig. A1 of M10). Moreover, we do not find any correlation between the power-law fraction given by H11 and the stellar masses or M_*/L_K derived by M10, which would be expected if the power-law features were biasing the M10 stellar mass estimates high.

Table 2. Stellar, gas and dynamical masses of SMGs (in units of $10^{11}\,M_\odot$).

SMG	$M_{*(M10)}{}^a$	$M_{*(C10)}{}^b$	$M_{*(H11)}{}^c$	M_{gas}	$M_{dyn}^{highCO\ d}$	$M_{dyn}^{CO(1-0)\ e}$
SMMJ123549.44+621536.8	$2.66^{+2.65}_{-1.33}$	$0.66^{+0.66}_{-0.33}$	$2.09^{+0.60}_{-0.47}$	2.07 ± 1.73^f	0.96 ± 0.44^g	2.30 ± 0.40^f
SMMJ123618.33+621550.5	$2.78^{+2.77}_{-1.39}$	$4.27^{+4.25}_{-2.13}$	$0.76^{+0.09}_{-0.08}$	0.35 ± 0.11^g	2.18 ± 0.18^g	4.36 ± 0.36^i
SMMJ123634.51+621241.0	$2.54^{+2.53}_{-1.27}$	$0.71^{+0.70}_{-0.35}$	$0.87^{+0.13}_{-0.11}$	0.25 ± 0.08^g	1.12 ± 0.25^g	2.24 ± 0.51^i
SMMJ123707.21+621408.1	$4.95^{+4.93}_{-2.47}$	$1.12^{+1.12}_{-0.56}$	$1.82^{+0.32}_{-0.27}$	1.69 ± 1.41^f	2.78 ± 1.05^g	2.20 ± 0.60^f
SMMJ131201.17+424208.1	$1.27^{+1.27}_{-0.63}$	$6.76^{+6.73}_{-3.37}$	$1.02^{+0.33}_{-0.25}$	1.34 ± 0.50^g	9.50 ± 2.38^g	19.01 ± 4.76^i
SMMJ163650.43+405734.5	$2.06^{+2.05}_{-1.03}$	$3.80^{+3.78}_{-1.90}$	$1.45^{+0.42}_{-0.32}$	2.56 ± 2.14^f	3.50 ± 1.79^g	4.10 ± 0.80^f
SMMJ163658.19+410523.8	$3.27^{+3.26}_{-1.63}$	$8.13^{+8.09}_{-4.05}$	$1.29^{+0.33}_{-0.26}$	2.95 ± 2.46^f	1.40 ± 0.88^g	5.80 ± 0.40^f
SMMJ163706.51+405313.8	$4.52^{+4.49}_{-2.25}$	$10.23^{+10.18}_{-5.10}$	$1.62^{+0.24}_{-0.21}$	0.24 ± 0.07^h	3.40^h	6.80^i
SMMJ221735.15+001537.2	$1.30^{+1.30}_{-0.65}$	$1.91^{+1.90}_{-0.95}$	$0.51^{+0.06}_{-0.06}$	0.30 ± 0.07^h	2.80^h	5.60^i

Notes. [a] Michałowski et al. (2010a) with Chabrier (2003) IMF. [b] From this work using the method of C10 for Bruzual & Charlot (2003) models and double SFH. [c] Hainline et al. (2011) for Bruzual & Charlot (2003) models. [d] Dynamical mass from high exitation CO line. [e] Dynamical mass from CO(1–0) line. [f] Ivison et al. (2011). [g] Engel et al. (2010). [h] Greve et al. (2005). [i] Obtained by multiplying the M_{dyn}^{highCO} by a factor of 2, the average correction from high excitation lines to CO(1–0) derived for four SMGs with CO(1–0) data. Mass errors for M10 and C10 are simply a factor of 2.

2.5.3. Lensing

If SMGs are lensed then the stellar masses derived by M10 and H11 should be corrected down. At least some of the brightest SMGs are thought to be lensed (Ivison et al. 1998; Downes & Solomon 2003; Dunlop et al. 2004; Kneib et al. 2004; Motohara et al. 2005; Wilson et al. 2008; Berciano Alba et al. 2010; Knudsen et al. 2010; Negrello et al. 2010; Swinbank et al. 2010b; Vieira et al. 2010; Tamura et al. 2010; Hezaveh & Holder 2011; Ikarashi et al. 2011). However, Lima et al. (2010, Fig. 2) found that the number counts of SMGs with $S_{850} < 20$ mJy do not require any lensing correction. Moreover, the modelling of Paciga et al. (2009, Fig. 6) showed that only $\lesssim 10\%$ of SMGs with $S_{850} < 15$ mJy at $z < 3$ are magnified by a factor of >2. Hence, the lensing correction for SMGs in the $850\,\mu$m flux-density range considered here is likely to be small on average.

3. Consistency tests for stellar masses

3.1. Dynamical masses

The estimates of the dynamical and H_2 gas masses from CO lines detected for SMGs provide a consistency check on the stellar mass estimates. Specifically, assuming that the extent of the CO-emitting gas is the same as the extent of the stellar component, the sum of the gas and stellar masses has to be less than the dynamical mass. Using this approach Engel et al. (2010) derived a mean ratio $(M_* + M_{gas})/M_{dyn} \simeq 2.1$ for seven SMGs using the stellar masses of M10 (corrected to the Chabrier 2003 IMF) and concluded that the stellar masses derived by M10 are inconsistent with their gas and dynamical masses. As explained below, we do not find that this is the case.

There is, of course, some uncertainty and controversy over the calculation of dynamical and molecular gas masses from CO line observations (e.g. Genzel et al. 2003; Ivison et al. 2011). Perhaps of most relevance for the present discussion is the fact that Engel et al. (2010) used high excitation lines (CO $J = 7–6$, 6–5, 4–3 and 3–2), which trace denser and hotter gas, very likely confined to the more central regions of a galaxy. Therefore, the derived dynamical masses could easily refer to regions smaller than the extent of the stellar component, making it difficult to compare them directly with the stellar masses. Indeed, based on low excitation CO(1–0) lines Ivison et al. (2011) found

dynamical masses higher by a factor $\simeq 2.4$–4.1 for two out of three SMGs, for which Engel et al. (2010) claimed a significant discrepancy between stellar and dynamical mass (HDF 76 and N2 850.2; the third one was not observed by Ivison et al.). Moreover, recently Riechers et al. (2011) found CO(1–0) sizes $\simeq 60$–90% larger than that reported by Engel et al. (2010) for two additional SMGs.

Interestingly, the mean CO half-light radius obtained by Engel et al. (2010) of 2.4 kpc is indeed 15–40% smaller than the typical half-light radius of the near-infrared emission dominated by the stellar component (2.8–3.4 kpc; Swinbank et al. 2010a; Mosleh et al. 2011; Targett et al. 2011). Moreover, one out of three SMGs for which Engel et al. (2010) claimed inconsistency with the M10 stellar mass (N2 850.2) was observed by Swinbank et al. (2010a) who measured the stellar extent to be $\simeq 3$ times larger than the extent of the CO(7–6) found by Engel et al. (2010). This reinforces the likelihood that the dynamical masses of the problematic SMGs have been under-estimated, as the stellar component is more extended than the high-excitation gas.

This argument is supported by hydrodynamical simulations of SMGs (Narayanan et al. 2009, 2010b; Hayward et al. 2011a,b), where only $\simeq 30\%$ of the stellar mass is distributed over the inner radius of 2.5 kpc, roughly the size over which Engel et al. (2010) calculated dynamical masses. This correction to the dynamical masses would be enough to remove the inconsistency with the stellar masses of M10, even though some simulations predict that the usual conversions result in the dynamical masses overpredicted by a factor of $\simeq 1.5$–1.9 (Narayanan et al. 2009, Fig. 10 and Eq. (6)).

In an attempt to overcome these systematics, and facilitate a fairer comparison of dynamical and stellar masses, we focus here on the newly available CO (1–0) dynamical masses which, as described above, appear to better trace the full extent of the SMGs, yielding somewhat larger sizes and masses. Stellar, gas and dynamical masses are available for 9 of the galaxies in our sample, including two CO detections made by Greve et al. (2005). These data[2] are presented in Table 2.

In the final column of this table we give the CO (1–0) dynamical mass as our best estimate of the dynamical mass of

---

[2] Note that Engel et al. (2010) used the stellar masses reported initially in Hainline (2008) whereas we quote the corrected values from H11.
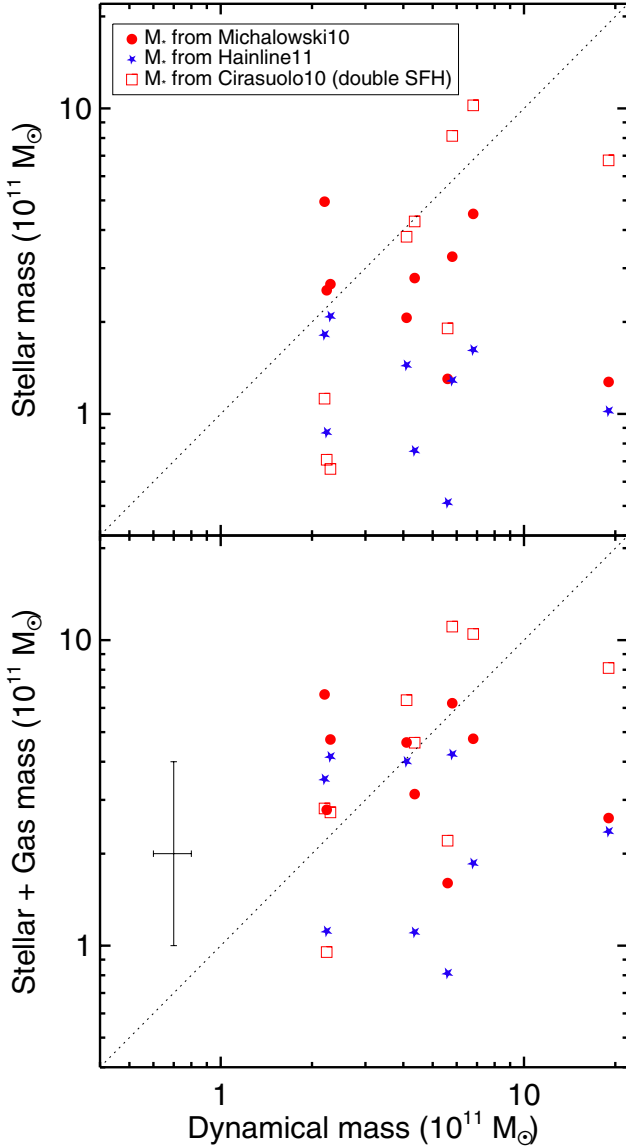
Fig. 3. Stellar mass (M_*) versus dynamical mass (M_{dyn}) estimated from CO(1–0) (*upper panel*), and stellar+H$_2$ gas mass ($M_* + M_{gas}$) versus M_{dyn} (*lower panel*) for the 9 SMGs for which the necessary results have been compiled in Table 2. The data points derived from the stellar mass estimates of H11 are indicated by *blue stars*, those based on the stellar mass estimates of M10 are indicated by *red circles*, while the new double-component C10 values are indicated by *red squares*. In principle, only the area below the *dotted line* represents a consistent set of galaxy properties with $M_{gas} + M_* \leq M_{dyn}$, but because of the typical scatter (indicated by the error bars in the lower panel) and unknown inclinations, ≃2–3 out of the 9 individual SMGs are in fact expected to exceed this apparent threshold (see Sect. 3.1 for details). We see that, contrary to the conclusion of Engel et al. (2010), there is no evidence that the stellar masses derived by M10 using the Chabrier IMF are in conflict with the dynamical mass estimates, even allowing for estimates of the additional gas mass. Indeed, the average values of these ratios favour the M10 stellar mass estimates as the most consistent with the available data (see Sect. 3.1).

each galaxy. Where available (4 SMGs) this number has been taken directly from the CO (1–0) observations performed by Ivison et al. (2011), while for the remaining objects this number has been inferred from the higher-order CO-line dynamical masses by multiplying them by the average correction factor for the aforementioned 4 SMGs for which the dynamical masses

of Ivison et al. (2011) and Engel et al. (2010) can be directly compared.

In Fig. 3 we then plot, for these 9 SMGs, M_* and also M_{gas} + M_* as a function of M_{dyn}, with the dynamical masses taken from the final column in Table 2, and the stellar mass estimates from H11, M10 and the present work (double-component C10 model) indicated by the different symbols.

From Fig. 3 it can be seen that, within the errors, there is no evidence that even the higher stellar mass determinations for any object exceed the estimated dynamical mass. At first sight it might seem that there could be more of a problem (for all mass determinations) for $M_* + M_{gas}$, but this is not really the case, both because of uncertainty in M_{gas}, and because of the potential effects of varying inclination angle on M_{dyn}. Specifically, while the unknown inclination (i) of gas discs should not influence the average $(M_{gas} + M_*)/M_{dyn}$ ratio, if the real inclination of an *individual* galaxy is lower than the assumed average, then its derived M_{dyn} is inevitably too low, which can make it *appear* to be inconsistent with the (orientation-independent) derived stellar mass. To quantify this effect we considered 100 000 galaxies with real $(M_{gas} + M_*)/M_{dyn} = 1$ (or 0.5) with inclinations distributed uniformly in three dimensions, i.e. with a mean $\langle \sin^2 i \rangle = 2/3$. We found that the adoption of this mean value for all galaxies results in ≃18% (9%) of them *appearing* to exceed the allowed $(M_{gas} + M_*)/M_{dyn} = 1$ by a factor of > 2 and ≃12% (7%) by a factor of >3. Hence, in a sample of ≃10 galaxies with random unknown inclinations, we would expect 1–2 of them to significantly exceed the allowed ratio, simply because of the unknown inclination of any molecular disc in an individual object.

In summary, one should expect, given the effects of random inclination and uncertainty in the measurement of M_*, M_{gas} and M_{dyn}, that a few galaxies should lie above the one-to-one relation indicated by the dotted line in Fig. 3, and it is the mean (or median) value of the mass ratios which need to be considered when reviewing the viability of the stellar masses. Working from the numbers given in Table 2, for the ratio M_*/M_{dyn} the mean (median) values are 0.36 (0.24) for the H11 stellar masses, 0.80 (0.64) for M10, and 0.94 (0.78) for the new double-component C10 values. Thus, adoption of the lower H11 stellar masses would imply that only ≃1/3 of the dynamical mass of a typical SMG can be accounted for by M_*. In contrast, the M10 and C10 results would imply that M_* for a typical SMG is ≃3/4 × M_{dyn}. If the values of M_{gas} in Table 2 are taken at face value then this latter scenario would appear to be more consistent with the data, as for the ratio $(M_* + M_{gas})/M_{dyn}$ the mean (median) values are 0.71 (0.50) for the H11 stellar masses, 1.15 (1.07) for M10, and 1.09 (1.19) for the new double-component C10 values. This then provides further evidence that the stellar mass estimates of H11 are a little too low, the new C10 double-component values are perhaps a little high, and the M10 results appear to provide the best description of the data.

We conclude that the latest estimates of the dynamical masses of SMGs are in very good accord with the stellar masses of SMGs estimated by M10 with the Chabrier (2003) IMF.

3.2. Number density of massive galaxies

Another consistency check on the plausibility of the stellar-mass estimates is to assess how the number density of SMGs compares with the number density of galaxies in general in the same implied stellar-mass range, at both lower and comparable redshifts.

Drory et al. (2004) reported the cumulative number density of galaxies $n(M_* > 1.1 \times 10^{11} M_\odot) = 3.16–0.64 \times 10^{-4}$ Mpc^{-3} at redshifts $z = 0.5–1.1$ (their Fig. 6 and Table 3, after conversion of their mass limit to the Chabrier 2003 IMF). Restricting the analysis to the SMGs at $z > 1.4$, and using the comoving volumes given by M10 we obtain $n_{SMG}(M_* > 1.1 \times 10^{11} M_\odot) = 7.0 \times 10^{-6}$ Mpc^{-3} for the M_* values of M10 and 3.8×10^{-6} Mpc^{-3} for the M_* values of H11. Hence, even for the M10 stellar mass estimates the number density of SMGs is $\simeq 30$ times lower than that of massive galaxies at lower redshifts and therefore the number of massive SMGs is clearly not inconsistent with the number density of massive galaxies at lower redshifts, even allowing for a relatively modest and plausible duty cycle (see below). In addition, from the mass comparisons discussed in the previous subsection, further conversion of the observed molecular gas reservoir into stars, even if extremely efficient, can at most increase the measured M10 stellar masses by $\simeq 30–50\%$ (or, equivalently, the H11 masses by $\simeq 100\%$), and so this basic conclusion is not seriously affected by potential further star formation.

The redshift range $1.4 < z < 3.6$ corresponds to a time interval of 2.7 Gyr. Given the typical gas reservoirs of $M_{gas} \simeq 1 \times 10^{11} M_\odot$ listed in Table 2 it can be seen that the typical gas exhaustion timescale is $\simeq 200$ Myr (assuming a typical SFR of $\simeq 500 M_\odot$ yr^{-1}). If one further assumes that a typical SMG is observed mid-way through its final violent star-forming peak, then a reasonable estimate of the submillimetre luminous lifetime of an SMG is 400 Myr (see also Bouché et al. 2005). This implies a duty-cycle number density correction factor of $\simeq 6–7$ for the redshift interval in question. If one further factors an incompleteness correction of a factor of $\simeq 3.5$ as derived by M10, then the implied true number density of *potential* SMGs in this era is close to, but still less than the best estimate of $M_* > 1.1 \times 10^{11} M_\odot$ galaxies at $z \simeq 1.1$. Hence, the conclusion that the stellar masses of SMGs are typically $M_* \simeq 2 \times 10^{11} M_\odot$ appears to be perfectly consistent with the number density of massive galaxies at $z \simeq 1$.

A similar conclusion can be reached comparing to the number density reported by Pozzetti et al. (2007, Fig. 11) and Kajisawa et al. (2009, Fig. 16): $n(M_* > 6 \times 10^{10} M_\odot) \simeq 10^{-3}–2 \times 10^{-4}$ Mpc^{-3} at $z = 0–2$, whereas the corresponding values for SMGs are $n_{SMG}(M_* > 6 \times 10^{10} M_\odot) = 8.7 \times 10^{-6}$ and 5.6×10^{-6} Mpc^{-3}.

Finally, we integrated the mass function at $z = 3–3.5$ given by Caputi et al. (2011) for $M_* > 10^{11} M_\odot$ galaxies, obtaining 7×10^{-6} Mpc^{-3}. This rather narrow redshift interval corresponds to an elapsed time of only 350 Myr, and so, following the above arguments, the duty cycle correction should be $\simeq$ unity. It is therefore perhaps unsurprising that this number density is rather similar to the number density of SMGs.

3.3. Numerical simulations of SMGs

Figure 4 shows submillimetre flux density versus stellar mass for a set of idealized hydrodynamic simulations of merging and isolated disk galaxies, where 3-D radiative transfer has been performed to calculate the submillimetre flux. The simulations are similar to those described in Narayanan et al. (2009, 2010a,b); see Hayward et al. (2011a,b) for a description of the differences. Note that the plot simply shows tracks for different simulations. No weighting by abundance has been applied, so only the range spanned by the simulations, not typical values, can be read from the plot.
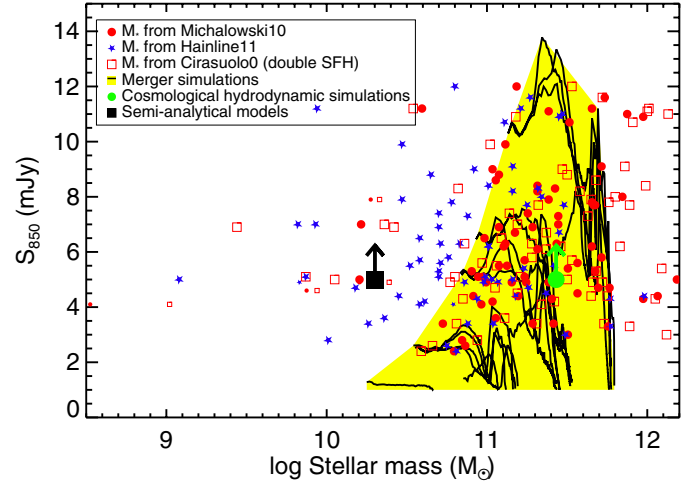
Fig. 4. Submillimetre flux densities as a function of the stellar masses of SMGs. *Solid lines* represent the evolutionary tracks from the merger hydrodynamic simulations (Narayanan et al. 2009, 2010a,b; Hayward et al. 2011a,b) enclosed in the *yellow shaded area*, *the big square* represents the median stellar mass of $2 \times 10^{10} M_\odot$ for SMGs with $S_{850} > 5$ mJy in the semi-analytical models (Baugh et al. 2005; Swinbank et al. 2008; González et al. 2011; Almeida et al. 2011), whereas *the big circle* corresponds to the median value derived by Davé et al. (2010) from the cosmological hydrodynamic simulations. Other symbols represent the observational data for SMGs with stellar masses from M10 (*red circles*), H11 (*blue stars*) and our new estimates based on C10 and double-component SFH (*red squares*). Small symbols indicate SMGs at $z < 0.5$. According to the hydrodynamic simulations, many of the stellar masses derived by H11 are too low to result in measurable submillimetre flux, while the stellar masses derived by M10 are consistent with the hydrodynamic simulation predictions (within the observational errors). Neither the H11, M10 or C10 stellar masses appear to agree, on average, with the median stellar mass predicted by the semi-analytic models.

We note that in order to reach $S_{850\,\mu m} \gtrsim 5$ mJy, these simulations require stellar mass to exceed $M_* \simeq 1 \times 10^{11} M_\odot$. As can be seen from Fig. 4, the predicted stellar mass range is in good agreement with the SMG stellar masses derived by M10. We note that, in the cold infall model of SMGs, comparably high stellar masses are also preferred (Davé et al. 2010, their Fig. 2).

On the other hand, the semi-analytical models of Baugh et al. (2005), Swinbank et al. (2008), González et al. (2011, Fig. 3) and Almeida et al. (2011) predict significantly lower stellar masses for SMGs, with a median $M_* \simeq 2 \times 10^{10} M_\odot$ (indicated by the square in Fig. 4). Such a value is lower even than the vast majority of the stellar masses derived by H11, confirming the findings of Swinbank et al. (2008) that the stellar masses of SMGs are generally systematically under-predicted by this class of semi-analytic model.

4. Specific star-formation rates

One important step towards locating SMGs within the general framework of galaxy/star formation at high redshift is to establish whether, on average, they simply represent the most massive extension of the normal star-forming galaxy population in the young active Universe at $z > 2$ (as predicted by Davé et al. 2010, in cosmological hydrodynamic simulations), or whether they are extreme outliers in terms of specific star-formation rate (sSFR).

To explore this we compare the properties of SMGs with other galaxies at similar redshifts as presented by Daddi et al. (2007, Fig. 17), Kajisawa et al. (2010, Fig. 2) and Rodighiero et al. (2011, Fig. 1).
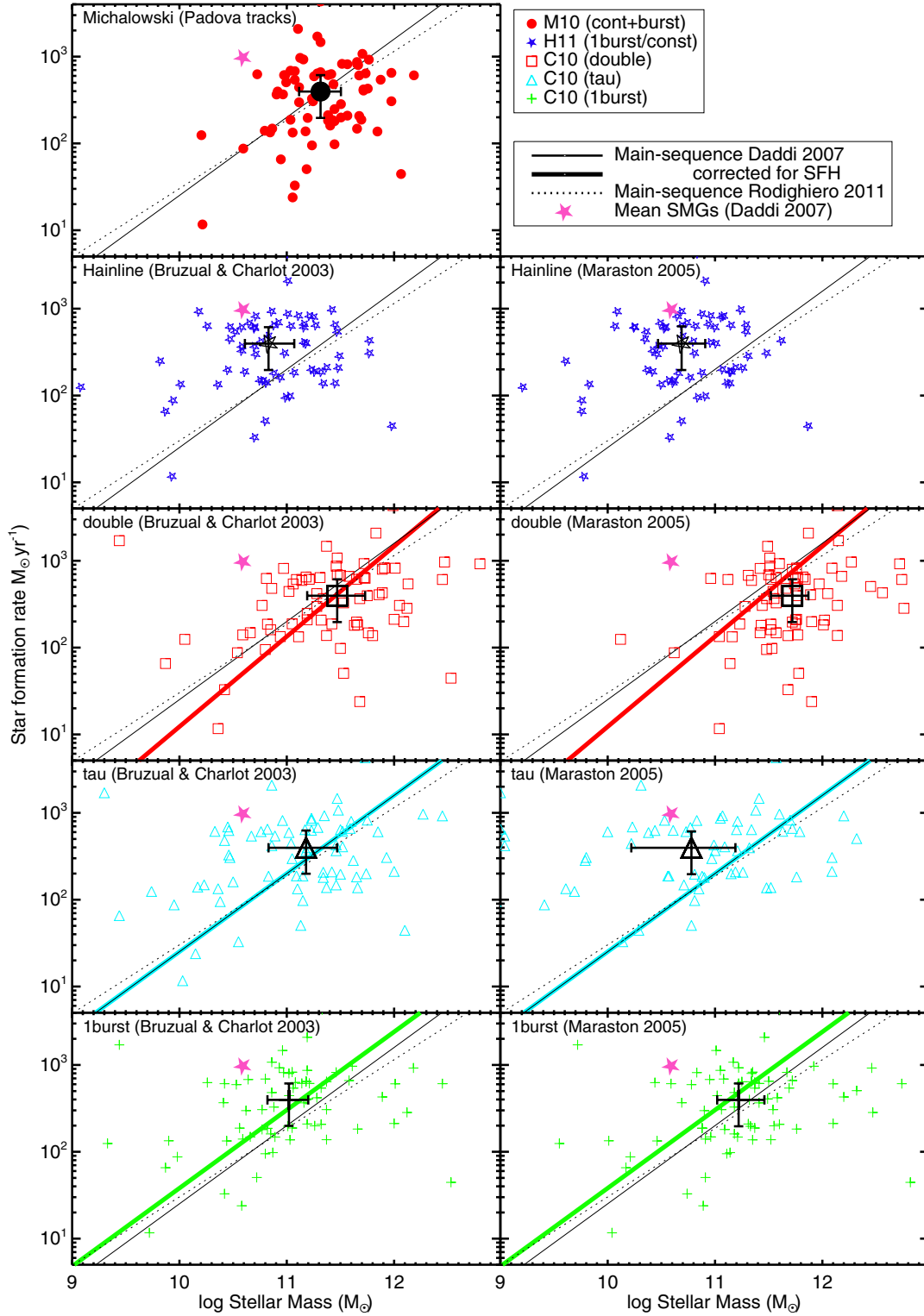
Fig. 5. SFRs of SMGs as a function of stellar masses derived using the stellar population synthesis models of Bruzual & Charlot (2003, *left*) and Maraston (2005, *right*). The symbols correspond to the stellar masses derived by M10 (*red circles*), H11 (*blue stars*) and our new estimates based on the SED modelling method of Cirasuolo et al. (2010, C10) for three alternative forms of star formation history (SFH): double-component model (*red squares*), exponentially-declining (tau) model (*light blue triangles*) and single burst (*green pluses*). The median values are shown as *large black symbols* with 3σ error bars. The "main-sequence" of star-forming galaxies at $z \simeq 2$ is shown as a *solid line* (Daddi et al. 2007) and *dotted line* (Rodighiero et al. 2011). The *thick, coloured solid lines* represent the "main-sequence" of Daddi et al. (2007) at $z \simeq 2$ corrected for the systematic difference in average stellar mass introduced by the self-consistent adoption of SFH to model SMGs in each panel (see Sect. 4 for details). All results have been converted to the Chabrier (2003) IMF. Unless the exponentially declining (tau model) SFH with the Maraston (2005) models are assumed, the SMGs are completely consistent with the high-mass end of this sequence. This agreement is essentially perfect for the M10 and double-component models. The *magenta star* shows the position of an average SMG as plotted by Daddi et al. (2007). Clearly, regardless of the assumed evolutionary stellar model or SFH, this supposed typical value of sSFR for SMGs is in fact unrepresentative of real SMGs.

For the SMGs we adopt the SFRs derived by M10 from the mid-far infrared emission. The comparison is shown in Fig. 5. Here, for the nine different determinations of SMG masses considered in this paper, we plot SFR versus M_* for all the individual SMGs in the sample, and compare the results with the location of the so-called "main-sequence" of star-forming galaxies at $z \simeq 2$ (Daddi et al. 2007; Rodighiero et al. 2011).

In order to ensure that this comparison is fair and self-consistent, we have also investigated how the choice of SFH influences the location of this "main-sequence". We assumed that the SFR estimate is independent of the adopted SFH (as it is usually derived from bolometric or monochromatic luminosity), and derived the stellar masses of all galaxies the UDS field in CANDELS (Grogin et al. 2011; Koekemoer et al. 2011) at $z = 1.5$–3 and $M_* = 10^{9.5}$–$10^{11.6}$ $M_\odot$ (Cirasuolo et al., in prep.) using the same SED fitting method outlined in Sect. 2.2 for double-burst, single-burst and tau SFHs. If we adopt the results of the single-burst models for these galaxies, we obtained masses consistently lower by 0.1 dex relative to those derived using the tau models; in Fig. 5 ("1 burst" panels) this is indicated by the position of the coloured thick line towards lower stellar masses. On the other hand, as expected, the adoption of the double-burst models yields higher stellar masses. However, this shift transpires to be mass-dependent; at 10^{10} $M_\odot$ the double-burst SFH produces stellar masses 0.3 dex higher than the tau SFH, whereas this shift is only 0.1 dex at $10^{11.5}$ $M_\odot$ (resulting in steepening of the thick line in the "double" panels). The latter is a significantly smaller shift than the 0.3 dex difference found between the double-burst and tau model stellar masses for SMGs (Table 1).

It is clear from this figure that, for almost all models the SMGs lie essentially exactly on this "main-sequence", within the errors. It is also clear that, even for the lower mass determinations, the average deviation from the "main-sequence" is relatively modest. As expected (given Table 1 and the discussion in Sect. 2.2), the offset is greatest for the exponentially-decreasing tau SFH with the Maraston (2005) models, but even then it can be seen that the majority of the SMGs are still actually consistent with the "main-sequence", and the formal $\simeq 3\sigma$ offset in average sSFR is in fact driven by a subset of extreme outliers. It can also be seen that none of the various determinations of SMG stellar masses yields a sSFR for a typical SMG as extreme as that claimed by Daddi et al. (2007). This discrepancy is likely because their stellar mass estimates are based on dynamical masses from high-excitation CO line observations (Tacconi et al. 2006), which may bias the stellar mass estimates low, as we explained in Sect. 3.1. Moreover, their use of infrared luminosity of $\sim 10^{13}$ $L_\odot$, estimated from a single $850\,\mu m$ detection (Greve et al. 2005; Tacconi et al. 2006), represents an overestimate, as revealed by recent *Herschel* studies (Magnelli et al. 2012; Roseboom et al. 2012, $\sim 10^{12.5-12.7}$ $L_\odot$) making the SFR estimate of Daddi et al. (2007) a factor of 2–3 too high.

To quantify the apparent consistency between the properties of SMGs and other star-forming galaxies at comparable epochs we report, in Table 1, the mean and median sSFRs for the SMGs as derived from the various alternative models (as stated above these values are IMF-independent). Again, with the possible exception of the Maraston (2005) tau-model, all the median values are clearly consistent with the values of a few Gyr^{-1} found by Daddi et al. (2007) and Kajisawa et al. (2010). Hence, it would appear that, while a few SMGs may be caught at unusually spectacular moments, in general it seems hard to avoid the conclusion that the SMG population is perfectly consistent with the high-mass end of the general star-forming galaxy population at these redshifts. Interestingly, it is only really the double-component

models which yield mean and median values which are formally consistent with each other, with the other models always producing a few extreme outliers with very low stellar masses. Thus, the use of the most physically plausible star-formation histories yields consistent and fairly well defined typical mean sSFR values for SMGs of $2-3$ Gyr^{-1}, in rather good agreement with the height of the plateau in sSFR at $z > 2$ discussed by González et al. (2010).

5. Conclusions

We have explored the potential origins of systematic differences in the stellar masses derived for SMGs, and have found that the difference between the stellar-mass estimates of M10 and H11 can be explained by the combination of different assumed IMFs, stellar population models and types of star formation histories. The available evidence supports the use of the Chabrier IMF (with the Salpeter IMF yielding excessive masses for several SMGs). The choice of which stellar synthesis model to adopt turns out to be relatively unimportant compared to the choice of star formation history. The one exception to this is the combination of an exponentially declining star formation history with the models of Maraston (2005), which produces radically different, unrealistically low stellar masses, presumably due to the very strong assumed TP-AGB contribution in these models.

For the same IMF and evolutionary synthesis model, the remaining difference between the average stellar mass estimates of M10 and H11 can be accounted for by differences in adopted star-formation history. Specifically, the two-component models of M10 yield values $\simeq 3$ times larger than the single-component models utilised by H11. We have explored this issue in more detail, by running further single-burst, tau-model and double-component model fits using the method of C10 and using both the Bruzual & Charlot (2003) and Maraston (2005) models. We find that the models which allow past and "present" star-formation activity to be disconnected yield very consistent average stellar masses in the range $M_* = 2-3 \times 10^{11}$ $M_\odot$, regardless of precisely how this is parameterized. We argue, therefore, that the main reason that authors such as H11 and Wardlow et al. (2011) have concluded in favour of typical SMG stellar masses $M_* < 1 \times 10^{11}$ $M_\odot$ is that they have assumed models in which the SFR in SMGs was always as high or higher prior to the epoch at which the object has been selected on the basis of its extreme star-formation activity. The more physically realistic two-component models are supported by other evidence for rising star-formation histories in star-forming galaxies at $z > 2$.

Considering potential orientation effects, and updated estimates of dynamical masses, we find that even the higher stellar mass estimates of M10 with the Chabrier IMF certainly cannot be excluded with current CO line data, and indeed yield total masses in good agreement with dynamical mass estimates. We also argue that SMG stellar masses $M_* \simeq 2 \times 10^{11}$ $M_\odot$ appear to be perfectly plausible given current measurements of the evolving mass function of the general galaxy population selected at near-infrared and mid-infrared wavelengths.

We also show that the mass estimates of M10 are in good agreement with the predictions of hydrodynamical merger models of SMGs and the cold inflow scenario, whereas those of H11 are closer to (but still not as low as) the much lower-mass predictions of certain semi-analytic models of galaxy formation.

Finally, we find that the inferred specific star-formation rates of SMGs are perfectly consistent with those derived for other star-forming galaxies at comparable redshifts, suggesting that most SMGs simply represent the high-mass extension of the "main-sequence" of star-forming galaxies at $z \geq 2$, and in

general should not be considered as outliers in the stellar mass-SFR relation.

References

Alexander, D. M., Bauer, F. E., Chapman, S. C., et al. 2005, ApJ, 632, 736
Alexander, D. M., Brandt, W. N., Smail, I., et al. 2008, AJ, 135, 1968
Almeida, C., Baugh, C. M., & Lacey, C. G. 2011, MNRAS, 417, 2057
Alongi, M., Bertelli, G., Bressan, A., et al. 1993, A&AS, 97, 851
Baugh, C. M., Lacey, C. G., Frenk, C. S., et al. 2005, MNRAS, 356, 1191
Berciano Alba, A., Koopmans, L. V. E., Garrett, M. A., Wucknitz, O., & Limousin, M. 2010, A&A, 509, A54
Bertelli, G., Bressan, A., Chiosi, C., Fagotto, F., & Nasi E. 1994, A&AS, 106, 275
Borys, C., Smail, I., Chapman, S. C., et al. 2005, ApJ, 635, 853
Bouché, N., Lehnert, M. D., & Péroux, C. 2005, MNRAS, 364, 319
Bressan, A., Fagotto, F., Bertelli, G., & Chiosi C. 1993, A&AS, 100, 647
Bruzual, G., & Charlot, S. 2003, MNRAS, 344, 1000
Bussmann, R. S., Dey, A., Armus, L., et al. 2012, ApJ, 744, 150
Cappellari, M., Bacon, R., Bureau, M., et al. 2006, MNRAS, 366, 1126
Caputi, K. I., Cirasuolo, M., Dunlop, J. S., et al. 2011, MNRAS, 413, 162
Chabrier, G. 2003, ApJ, 586, L133
Chapman, S. C., Blain, A. W., Smail, I., & Ivison, R. J. 2005, ApJ, 622, 772
Cimatti, A., Cassata, P., Pozzetti, L., et al. 2008, A&A, 482, 21
Cirasuolo, M., McLure, R. J., Dunlop, J. S., et al. 2007, MNRAS, 380, 585
Cirasuolo, M., McLure, R. J., Dunlop, J. S., et al. 2010, MNRAS, 401, 1166
Conroy, C., & Gunn, J. E. 2010, ApJ, 712, 833
Coppin, K., Chapin, E. L., Mortier, A. M. J., et al. 2006, MNRAS, 372, 1621
Daddi, E., Dickinson, M., Morrison, G., et al. 2007, ApJ, 670, 156
Davé, R., Finlator, K., Oppenheimer, B. D., et al. 2010, MNRAS, 404, 1355
Downes, D., & Solomon, P. M. 2003, ApJ, 582, 37
Drory, N., Bender, R., Feulner, G., et al. 2004, ApJ, 608, 742
Dunlop, J. S., McLure, R. J., Yamada, T., et al. 2004, MNRAS, 350, 769
Dye, S., Eales, S. A., Aretxaga, I., et al. 2008, MNRAS, 386, 1107
Dye, S., Eales, S. A., Moncelsi, L., & Pascale, E. 2010, MNRAS, 407, L69
Eminian, C., Kauffmann, G., Charlot, S., et al. 2008, MNRAS, 384, 930
Engel, H., Tacconi, L. J., Davies, R. I., et al. 2010, ApJ, 724, 233
Erb, D. K., Steidel, C. C., Shapley, A. E., et al. 2006, ApJ, 646, 107
Fagotto, F., Bressan, A., Bertelli, G., & Chiosi, C. 1994a, A&AS, 104, 365
Fagotto, F., Bressan, A., Bertelli, G., & Chiosi, C. 1994b, A&AS, 105, 29
Fagotto, F., Bressan, A., Bertelli, G., & Chiosi, C. 1994c, A&AS, 105, 39
Finlator, K., Oppenheimer, B. D., & Davé, R. 2011, MNRAS, 410, 1703
Fontanot F., Monaco P., Silva L., & Grazian A. 2007, MNRAS, 382, 903
Genzel, R., Baker, A. J., Tacconi, L. J., et al. 2003, ApJ, 584, 633
Gerhard, O., Kronawitter, A., Saglia, R. P., & Bender, R. 2001, AJ, 121, 1936
Girardi, L., Bressan, A., Chiosi, C., Bertelli, G., & Nasi, E. 1996, A&AS, 117, 113
Girardi, L., Bressan, A., Bertelli, G., & Chiosi, C. 2000, A&AS, 141, 371
González, V., Labbé, I., Bouwens, R. J., et al. 2010, ApJ, 713, 115
González, J. E., Lacey, C. G., Baugh, C. M., & Frenk, C. S. 2011, MNRAS, 413, 749
Greve, T. R., Bertoldi, F., Smail, I., et al. 2005, MNRAS, 359, 1165
Grillo, C., Gobat, R., Lombardi, M., & Rosati, P. 2009, A&A, 501, 461
Grogin, N. A., Kocevski, D. D., Faber, S. M., et al. 2011, ApJS, 197, 35
Hainline, L. J. 2008, Multi-Wavelength Properties of Submillimeter-Selected Galaxies, Ph.D. Thesis, California Institute of Technology
Hainline, L. J., Blain, A. W., Smail, I., et al. 2009, ApJ, 699, 1610
Hainline, L. J., Blain, A. W., Smail, I., et al. 2011, ApJ, 740, 96
Hatsukade, B., Iono, D., Akiyama, T., et al. 2010, ApJ, 711, 974
Hayward, C. C., Kereš, D., Jonsson, P., et al. 2011a, ApJ, 743, 159
Hayward, C. C., Narayanan, D., Jonsson, P., et al. 2011b, ASP Conf. Ser., 440, 369
Hayward, C. C., Jonsson, P., Kereš, D., et al. 2012, MNRAS, submitted [arXiv:1203.1318]

Henriques, B., Maraston, C., Monaco, P., et al. 2011, MNRAS, 415, 3571
Hezaveh, Y. D., & Holder, G. P. 2011, ApJ, 734, 52
Iglesias-Páramo, J., Buat, V., Hernández-Fernández, J., et al. 2007, ApJ, 670, 279
Ikarashi, S., Kohno, K., Aguirre, J. E., et al. 2011, MNRAS, 415, 3081
Ivison, R. J., Smail, I., Le Borgne, J. F., et al. 1998, MNRAS, 298, 583
Ivison, R. J., Papadopoulos, P. P., Smail, I., et al. 2011, MNRAS, 412, 1913
Kajisawa, M., Ichikawa, T., Tanaka, I., et al. 2009, ApJ, 702, 1393
Kajisawa, M., Ichikawa, T., Yamada, T., et al. 2010, ApJ, 723, 129
Kneib, J., van der Werf, P. P., Kraiberg Knudsen, K., et al. 2004, MNRAS, 349, 1211
Knudsen, K. K., Kneib, J., Richard, J., Petitpas, G., & Egami, E. 2010, ApJ, 709, 210
Koekemoer, A. M., Faber, S. M., Ferguson, H. C., et al. 2011, ApJS, 197, 36
Kriek, M., Labbé, I., Conroy, C., et al. 2010, ApJ, 722, L64
Kroupa, P. 2001, MNRAS, 322, 231
Lima, M., Jain, B., Devlin, M., & Aguirre, J. 2010, ApJ, 717, L31
MacArthur, L. A., McDonald, M., Courteau, S., & Jesús González, J. 2010, ApJ, 718, 768
Magnelli, B., Lutz, D., Santini, P., et al. 2012, A&A, 539, A155
Maraston, C. 2005, MNRAS, 362, 799
Maraston, C., Daddi, E., Renzini, A., et al. 2006, ApJ, 652, 85
Maraston, C., Pforr, J., Renzini, A., et al. 2010, MNRAS, 407, 830
Menéndez-Delmestre, K., Blain, A. W., Alexander, D. M., et al. 2007, ApJ, 655, L65
Menéndez-Delmestre, K., Blain, A. W., Smail, I., et al. 2009, ApJ, 699, 667
Michałowski, M., Hjorth, J., & Watson, D. 2010a, A&A, 514, A67
Michałowski, M. J., Watson, D., & Hjorth, J. 2010b, ApJ, 712, 942
Mosleh, M., Williams, R. J., Franx, M., & Kriek, M. 2011, ApJ, 727, 5
Motohara, K., Takata, T., Iwamuro, F., et al. 2005, AJ, 129, 53
Murphy, E. J., Chary, R. R., Alexander, D. M., et al. 2009, ApJ, 698, 1380
Narayanan, D., Cox, T. J., Hayward, C. C., Younger, J. D., & Hernquist, L. 2009, MNRAS, 400, 1919
Narayanan, D., Dey, A., Hayward, C. C., et al. 2010a, MNRAS, 407, 1701
Narayanan, D., Hayward, C. C., Cox, T. J., et al. 2010b, MNRAS, 401, 1613
Negrello, M., Hopwood, R., De Zotti, G., et al. 2010, Science, 330, 800
Noeske, K. G., Weiner, B. J., Faber, S. M., et al. 2007, ApJ, 660, L43
Paciga, G., Scott, D., & Chapin, E. L. 2009, MNRAS, 395, 1153
Papovich C., Finkelstein S. L., Ferguson H. C., Lotz J. M., & Giavalisco M. 2011, MNRAS, 412, 1123
Pope, A., Chary, R. R., Alexander, D. M., et al. 2008, ApJ, 675, 1171
Pozzetti, L., Bolzonella, M., Lamareille, F., et al. 2007, A&A, 474, 443
Ricciardelli, E., Trujillo, I., Buitrago, F., & Conselice, C. J. 2010, MNRAS, 406, 230
Riechers, D. A., Hodge, J., Walter, F., Carilli, C. L., & Bertoldi, F. 2011, ApJ, 739, L31
Rodighiero, G., Daddi, E., Baronchelli, I., et al. 2011, ApJ, 739, L40
Roseboom, I. G., Ivison, R. J., Greve, T. R., et al. 2012, MNRAS, 419, 2758
Salpeter, E. E. 1955, ApJ, 121, 161
Santini, P., Maiolino, R., Magnelli, B., et al. 2010, A&A, 518, L154
Schael, A. M. 2009, The Star-Formation History of Massive Galaxies, Ph.D. Thesis, University of Edinburgh
Silva, L., Granato, G. L., Bressan, A., & Danese, L. 1998, ApJ, 509, 103
Swinbank, A. M., Lacey, C. G., Smail, I., et al. 2008, MNRAS, 391, 420
Swinbank, A. M., Smail, I., Chapman, S. C., et al. 2010a, MNRAS, 405, 234
Swinbank, A. M., Smail, I., Longmore, S., et al. 2010b, Nature, 464, 733
Tacconi, L. J., Neri, R., Chapman, S. C., et al. 2006, ApJ, 640, 228
Tamura, Y., Iono, D., Wilner, D. J., et al. 2010, ApJ, 724, 1270
Targett, T. A., Dunlop, J. S., McLure, R. J., et al. 2011, MNRAS, 412, 295
Taylor, M. B. 2005, in Astronomical Data Analysis Software and Systems XIV, ed. P. Shopbell, M. Britton, & R. Ebert, ASP Conf. Ser., 347, 29
Thomson, M. G., & Chary, R. R. 2011, ApJ, 731, 72
Valiante, E., Lutz, D., Sturm, E., et al. 2007, ApJ, 660, 1060
van der Wel, A., Franx, M., van Dokkum, P. G., et al. 2006a, ApJ, 636, L21
van der Wel, A., Franx, M., Wuyts, S., et al. 2006b, ApJ, 652, 97
van Dokkum, P. G. 2008, ApJ, 674, 29
van Dokkum, P. G., & Conroy, C. 2010, Nature, 468, 940
van Dokkum, P. G., & Conroy, C. 2011, ApJ, 735, L13
Vieira, J. D., Crawford, T. M., Switzer, E. R., et al. 2010, ApJ, 719, 763
Wardlow, J. L., Smail, I., Coppin, K. E. K., et al. 2011, MNRAS, 415, 1479
Watabe, Y., Risaliti, G., Salvati, M., et al. 2009, MNRAS, 396, L1
Weidner, C., Kroupa, P., & Pflamm-Altenburg, J. 2011, MNRAS, 412, 979
Wilson, G. W., Hughes, D. H., Aretxaga, I., et al. 2008, MNRAS, 390, 1061
Zibetti, S., Charlot, S., & Rix, H. 2009, MNRAS, 400, 1181
Zibetti, S., Gallazzi, A., Charlot, S., Pasquali, A., & Pierini, D. 2012, [arXiv:1203.4571]

Appendix A: Table with all stellar mass estimates

Table A.1. Stellar masses of individual SMGs calculated using various methods, stellar population models and star formation histories.

		M_* (log $M_\odot$)								
SMG	z	M10[a] Padova double	H11[b] BC03 single	H11[c] M05 single	C10[d] BC03 1burst	C10[e] BC03 tau	C10[f] BC03 2burst	C10[g] M05 1burst	C10[h] M05 tau	C10[i] M05 2burst
SMMJ030226.17+000624.5	0.080	10.275	−99.000	−99.000	10.010	10.000	10.330	9.810	9.810	10.590
SMMJ030227.73+000653.5	1.408	10.915	11.180	11.009	11.180	11.190	11.750	11.320	11.320	11.770
SMMJ030231.81+001031.3	1.316	10.205	9.080	9.209	9.330	9.740	10.050	9.550	9.690	10.120
SMMJ030236.15+000817.1	2.435	11.285	10.880	10.689	11.180	11.170	11.310	11.250	11.200	11.570
SMMJ030238.62+001106.3	0.276	8.525	10.790	10.639	8.220	8.520	9.020	8.520	7.200	9.480
SMMJ030244.82+000632.3	0.176	10.205	9.830	9.559	10.100	10.090	10.390	9.950	9.950	10.410
SMMJ105151.69+572636.0	1.147	11.175	11.450	11.109	11.370	11.370	11.370	11.520	11.520	12.140
SMMJ105155.47+572312.7	2.686	11.235	10.580	10.419	10.880	10.460	11.530	11.180	8.650	11.570
SMMJ105158.02+571800.2	2.239	11.675	11.480	11.259	11.320	11.340	11.320	11.600	11.260	12.020
SMMJ105200.22+572420.2	0.689	10.945	9.870	9.759	9.870	9.440	9.870	10.170	7.630	11.140
SMMJ105201.25+572445.7	2.148	11.115	10.470	10.349	11.020	11.040	11.020	11.020	10.220	11.540
SMMJ105207.49+571904.0	2.689	11.655	11.010	10.879	11.190	11.230	11.460	11.050	11.050	11.510
SMMJ105225.79+571906.4	2.372	11.385	11.070	10.879	11.660	11.650	11.660	11.760	11.760	12.010
SMMJ105227.58+572512.4	2.142	11.565	11.370	11.189	11.190	11.420	11.190	11.310	11.190	11.750
SMMJ105227.77+572218.2	1.956	11.445	9.820	9.609	−99.000	−99.000	11.190	−99.000	−99.000	−99.000
SMMJ105230.73+572209.5	2.611	11.875	11.470	11.289	11.320	10.890	12.130	11.690	9.040	11.970
SMMJ105238.19+571651.1	1.852	10.905	10.700	10.519	11.160	11.460	11.680	11.410	11.210	11.480
SMMJ105238.30+572435.8	3.036	11.975	11.450	11.289	11.180	10.820	11.180	11.500	9.000	11.820
SMMJ123549.44+621536.8	2.203	11.425	11.320	11.149	10.820	10.830	10.820	10.880	10.880	11.520
SMMJ123553.26+621337.7	2.098	11.075	10.650	10.489	10.640	11.290	11.500	10.950	10.770	11.310
SMMJ123555.14+620901.7	1.875	11.505	11.230	11.069	11.260	11.740	12.090	11.550	11.150	11.900
SMMJ123600.10+620253.5	2.710	11.285	−99.000	−99.000	9.440	9.300	9.440	9.720	9.000	12.150
SMMJ123600.15+621047.2	1.994	11.385	10.470	10.249	11.140	11.520	11.650	11.410	11.630	11.840
SMMJ123606.72+621550.7	2.416	11.195	10.450	10.369	11.010	11.500	11.650	11.330	10.810	11.720
SMMJ123606.85+621021.4	2.509	11.735	11.270	11.149	11.370	11.500	11.720	11.340	11.340	11.750
SMMJ123616.15+621513.7	2.578	11.715	10.760	10.799	11.280	10.860	11.280	11.580	9.040	12.050
SMMJ123618.33+621550.5	1.865	11.445	10.880	10.659	10.770	11.340	11.630	11.090	10.900	11.430
SMMJ123621.27+621708.4	1.988	11.655	10.780	10.619	10.890	11.460	11.760	11.210	10.710	11.570
SMMJ123622.65+621629.7	2.466	11.665	11.250	11.059	11.020	11.600	11.890	11.340	11.210	11.720
SMMJ123629.13+621045.8	1.013	11.445	11.030	10.909	10.870	11.150	11.500	11.140	10.810	11.530
SMMJ123632.61+620800.1	1.993	11.075	10.520	10.359	11.060	10.670	11.060	11.370	8.830	11.740
SMMJ123634.51+621241.0	1.219	11.405	10.940	10.769	10.850	10.500	10.850	11.180	8.610	11.520
SMMJ123635.59+621424.1	2.005	11.125	11.420	11.239	11.610	12.270	12.470	11.920	11.600	12.270
SMMJ123636.75+621156.1	0.557	10.215	9.930	9.779	9.720	10.030	10.360	10.040	8.480	11.040
SMMJ123651.76+621221.3	0.298	9.875	−99.000	−99.000	9.430	9.590	9.940	9.510	8.650	10.230
SMMJ123707.21+621408.1	2.484	11.695	11.260	11.139	11.050	11.090	11.050	11.370	10.570	11.750
SMMJ123711.98+621325.7	1.992	11.035	10.610	10.419	10.560	11.150	11.420	10.880	10.560	11.230
SMMJ123712.05+621212.3	2.914	11.845	11.340	11.139	11.030	11.660	11.800	11.350	11.480	11.680
SMMJ123716.01+620323.3	2.037	11.675	−99.000	−99.000	12.010	11.850	13.150	12.100	10.000	13.100
SMMJ123721.87+621035.3	0.979	11.185	10.800	10.689	10.720	11.130	11.530	10.910	10.780	11.780
SMMJ131201.17+424208.1	3.405	11.105	11.010	10.909	11.190	10.860	11.830	11.460	10.310	11.870
SMMJ131208.82+424129.1	1.544	11.245	10.980	10.809	10.770	10.470	10.770	11.060	9.800	11.440
SMMJ131212.69+424422.5	2.805	11.565	10.710	10.649	10.970	10.960	10.970	10.830	10.830	11.420
SMMJ131215.27+423900.9	2.565	12.065	11.980	11.869	12.530	12.100	12.530	12.820	10.290	13.220
SMMJ131222.35+423814.1	2.565	11.505	11.490	11.309	12.120	11.620	12.120	12.470	9.790	12.760
SMMJ131225.20+424344.5	1.038	10.795	10.810	10.609	10.590	10.170	10.590	10.910	8.340	11.770
SMMJ131225.73+423941.4	1.554	10.965	10.580	10.469	10.410	11.180	11.340	10.690	11.000	11.550
SMMJ131228.30+424454.8	2.931	11.415	11.040	10.819	11.080	11.230	11.730	11.370	10.610	11.770
SMMJ131231.07+424609.0	2.713	10.995	−99.000	−99.000	15.890	15.330	13.360	12.320	12.320	12.450
SMMJ131232.31+423949.5	2.320	11.765	10.180	10.089	12.180	12.450	12.800	12.460	12.200	12.720
SMMJ131239.14+424155.7	2.242	11.255	10.700	10.529	10.530	11.020	11.140	10.780	10.380	11.340
SMMJ141741.81+522823.0	1.150	11.755	11.770	11.619	11.890	11.460	11.890	12.200	10.990	12.560
SMMJ141742.04+523025.7	0.661	10.865	10.750	10.569	10.660	10.230	10.660	10.960	8.410	11.420
SMMJ141750.50+523101.0	2.128	10.845	10.010	9.829	9.900	10.360	10.940	10.010	9.610	11.040
SMMJ141800.40+512820.3	1.913	12.185	11.160	10.999	12.450	13.620	12.450	12.740	11.790	12.740
SMMJ141802.87+523011.1	2.127	10.725	10.260	10.069	10.260	10.460	10.810	10.440	10.440	10.960
SMMJ141809.00+522803.8	2.712	11.975	11.770	11.479	11.370	11.930	12.050	11.540	12.090	12.140
SMMJ141813.54+522923.4	3.484	11.055	10.360	10.499	10.440	11.100	11.110	10.460	10.850	11.160

Table A.1. continued.

SMG	z	M10[a] Padova double	H11[b] BC03 single	H11[c] M05 single	C10[d] BC03 1burst	C10[e] BC03 tau	C10[f] BC03 2burst	C10[g] M05 1burst	C10[h] M05 tau	C10[i] M05 2burst
						M_* (log $M_\odot$)				
SMMJ163627.94+405811.2	3.180	10.985	10.580	10.249	10.420	10.760	11.090	10.590	10.730	11.120
SMMJ163631.47+405546.9	2.283	11.435	10.830	10.699	10.860	10.420	10.860	11.180	8.610	11.660
SMMJ163639.01+405635.9	1.495	10.975	10.700	10.539	11.210	10.330	11.210	11.220	8.510	11.520
SMMJ163650.43+405734.5	2.378	11.315	11.160	10.939	11.580	11.590	11.580	11.720	11.720	12.180
SMMJ163658.19+410523.8	2.454	11.515	11.110	10.959	11.050	11.750	11.910	11.350	11.700	11.760
SMMJ163658.78+405728.1	1.190	11.235	10.990	10.839	10.800	10.380	10.800	11.110	8.960	11.480
SMMJ163704.34+410530.3	0.840	10.595	9.940	9.759	9.980	9.950	10.540	10.210	9.410	10.620
SMMJ163706.51+405313.8	2.374	11.655	11.210	11.079	11.460	11.230	12.010	11.670	10.530	12.090
SMMJ221724.69+001242.1	0.510	11.055	−99.000	−99.000	10.580	10.150	11.680	10.890	8.340	11.900
SMMJ221725.97+001238.9	3.094	11.705	−99.000	−99.000	10.860	11.480	11.470	11.170	11.380	11.510
SMMJ221733.02+000906.0	0.926	11.385	−99.000	−99.000	12.000	12.000	12.000	12.100	12.090	11.760
SMMJ221733.12+001120.2	0.652	11.075	10.700	10.579	10.420	10.550	10.420	10.740	10.140	11.680
SMMJ221733.91+001352.1	2.555	11.715	11.160	10.959	11.200	11.520	11.860	11.490	11.090	11.890
SMMJ221735.15+001537.2	3.098	11.115	10.710	10.459	10.620	11.050	11.280	10.900	10.970	11.280
SMMJ221735.84+001558.9	3.089	11.155	10.860	10.689	10.930	11.350	11.720	11.220	11.070	11.600
SMMJ221737.39+001025.1	2.614	11.315	−99.000	−99.000	10.960	11.470	11.370	11.010	11.410	11.490
SMMJ221804.42+002154.4	2.517	11.035	10.920	10.739	10.800	10.450	11.470	11.080	10.230	11.500
SMMJ221806.77+001245.7	3.623	11.315	11.010	10.839	11.330	11.730	11.990	11.600	11.570	12.140

Notes. The Chabrier (2003) IMF is assumed. −99 indicates the lack of an estimate for a given SMG. [a] Stellar mass derived by M10. [b] Stellar mass derived by H11 with BC03 models. [c] Stellar mass derived by H11 with M05 models. [d] Stellar mass derived as in C10 with BC03 models and single-burst SFH. [e] Stellar mass derived as in C10 with BC03 models and tau SFH. [f] Stellar mass derived as in C10 with BC03 models and double-burst SFH. [g] Stellar mass derived as in C10 with M05 models and single-burst SFH. [h] Stellar mass derived as in C10 with M05 models and tau SFH. [i] Stellar mass derived as in C10 with M05 models and double-burst SFH. References: M10 (Michałowski et al. 2010a); H11 (Hainline et al. 2011); C10 (Cirasuolo et al. 2010); BC03 (Bruzual & Charlot 2003); M05 (Maraston 2005).